The Marshall Grazing Incidence X-ray Spectrometer

Ken Kobayashi[a], Amy R. Winebarger[a], Sabrina Savage[a], Patrick Champey[a], Peter N. Cheimets[b], Edward Hertz[b], Alexander R. Bruccoleri[c], Jorg Scholvin[c], Leon Golub[d], Brian Ramsey[a], Jaganathan Ranganathan[a], Vanessa Marquez[b], Ryan Allured[b], Theodore Parker[b], Ralf K. Heilmann[d], and Mark L. Schattenburg[d]

[a]NASA Marshall Space Flight Ctr. Huntsville, AL 35812, USA
[b]Smithsonian Astrophysical Observatory, Cambridge, MA 02138, USA
[c]Izentis LLC, PO Box 397002, Cambridge, MA 02139, USA
[d]Massachusetts Institute of Technology, Cambridge, MA 02139, USA

ABSTRACT

The Marshall Grazing Incidence X-ray Spectrometer (MaGIXS) is a NASA sounding rocket instrument designed to obtain spatially resolved soft X-ray spectra of the solar atmosphere in the 6–24 Å (0.5–2.0 keV) range. The instrument consists of a single shell Wolter Type-I telescope, a slit, and a spectrometer comprising a matched pair of grazing incidence parabolic mirrors and a planar varied-line space diffraction grating. The instrument is designed to achieve a 50 mÅ spectral resolution and 5 arcsecond spatial resolution along a ±4-arcminute long slit, and launch is planned for 2019. We report on the status and our approaches for fabrication and alignment for this novel optical system. The telescope and spectrometer mirrors are replicated nickel shells, and are currently being fabricated at the NASA Marshall Space Flight Center. The diffraction grating is currently under development by the Massachusetts Institute of Technology (MIT); because of the strong line spacing variation across the grating, it will be fabricated through e-beam lithography.

1. INTRODUCTION

The solar corona is a high temperature plasma in the 10^6 to 10^7 K range and radiates predominantly in the soft X-ray range. Efforts to understand the plasma temperature distribution have been hampered by the limitations of the observations. Soft X-ray spectrometers flown in the past, such as the Bragg Crystal Spectrometer (BCS[1]) on the Yohkoh satellite, could only observe the average spectra over a fairly large field of view.[2] Soft X-ray imaging telescopes such as the X-Ray Telescope[3] on the Hinode satellite have limited energy diagnostic capabilities, and can only determine an approximate temperature by taking filter ratios through multiple broadband filters.

MaGIXS is designed to provide the first spatially resolved soft X-ray spectra of the solar corona (see Figure 1 for the full simulated spectrum). The ability to measure the temperature distribution at different parts of a solar active region will help to resolve the debate concerning the heating mechanism and frequency of active region coronal loops, which is not sufficiently achievable with currently-available instrumentation. MaGIXS will also be able to provide strong constraints on the variability of elemental abundance in the active region due to the inclusion of key first ionization potential (FIP) diagnostic lines in the observed spectrum.

MaGIXS has been selected for a NASA sounding rocket flight, currently scheduled for summer of 2019. Mechanical design and mirror fabrication are underway.

2. GOALS AND OBJECTIVES

There are two main scientific objectives for MaGIXS. The first is to determine the nature of active region heating events through temperature diagnostics of the high-temperature corona. Extreme ultraviolet (EUV) spectrographs currently operating (e.g. EUV Imaging Spectrometer[4] on the Hinode satellite) provide accurate measurements of the differential emission measure (DEM) up to $Log\,T = 6.8$ range. However, determination of DEM up to higher temperatures requires observation of higher temperature lines.[5] A grazing-incidence

Send correspondence to K.K.: E-mail: ken.kobayashi@nasa.gov, Telephone: (+1) 256-961-7644

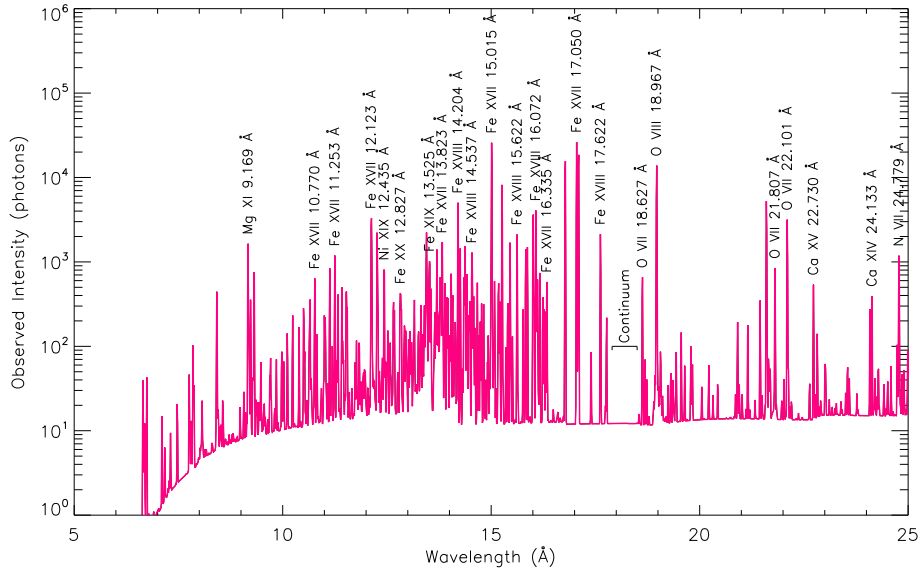

Spectral Line		Log T
Fe XX	12.85 Å	7.0
Fe XIX	13.53 Å	6.8
Fe XVIII	14.21 Å	6.8
Fe XVII	15.01 Å	6.6
Mg XII	8.42 Å	6.9
Mg XI	9.16 Å	6.4
Ne X	12.13 Å	6.6
Ne IX	13.45 Å	6.2
O VIII	18.97 Å	6.4
O VII	21.60 Å	6.3

Figure 1. Simulated MaGIXS active region spectrum (left), and list of lines required to be observed to meet science requirements (right).

spectrograph designed to cover a wavelength range of 10–23 Å is capable of measuring coronal DEM up to $Log\,T = 7.3$. This bandwidth provides a strong constraint on the heating mechanism of the corona.

The second science objective is to measure the variation of elemental abundance in solar active region structures. The same 9–23 Å wavelength coverage includes the emission lines from a number of key diagnostic elements, including Mg, Ne, Fe, and O (Figure 1). This set of lines allows MaGIXS to measure how elemental abundance varies across the active region as a function of first ionization potential (FIP).

The performance requirements to meet these scientific goals are listed in Table 1, along with design constraints. MaGIXS is designed as a sounding rocket experiment, with use of a NASA sounding rocket (e.g. Black Brant IX) in mind. The spatial resolution requirement is set as the minimum necessary to resolve coronal loop structures. While the size of the smallest loop structures is unknown, 5-arcsecond resolution is sufficient to resolve the overall magnetic field structure of an active region. The field of view is set as the size of a typical active region. The wavelength range has been increased so that second-order contamination lines can also be observed and identified in the first order.

Table 1. Requirements and constraints for MaGIXS.

	requirement	baseline design
Wavelength Range	9–22Å	6–24Å
Wavelength Resolution	50 mÅ	50 mÅ(10 mÅ/pixel)
Spatial Resolution	5.0″	5.0″ (2.5″/pixel)
Slit length	> 5.0 arcmin	8 arcmin
Detector Pixel Size		$13 \times 13\,\mu$m
Instrument Length	~ 3.3 m	3.3 m
Effective Area	5 mm^2 peak	5 mm^2 peak

3. OPTICAL DESIGN

The optical design[6] is a fully grazing-incidence telescope and spectrograph, as shown in Figure 2. The telescope is a conventional Wolter-I design with a 1.09 m focal length and 1.0° graze angle. A slit samples a 2.5-arcsec wide strip from the focused image. The spectrograph consists of paired, identical grazing-incidence parabolic mirrors followed by a planar varied line space grating. The spectrograph mirrors have graze angles of 2.0° to match the exit cone angle of the telescope. Two spectrograph mirrors are necessary to suppress off-axis aberration (coma) by approximately meeting the Abbe sine condition, thus achieving the required resolution for the entire slit. The diffraction grating is in a convergent beam, and the ruling frequency is varied from 1850 to 2500 lines/mm across the 73 mm long grating to correct for astigmatism

4. INSTRUMENT DESIGN & ALIGNMENT PLAN

The instrument consists of 4 sub-assemblies as shown in Figure 3: the Telescope Mirror Assembly (TMA), the slit/slitjaw assembly, the Spectrograph Optics Assembly (SOA, containing the spectrograph mirrors + grating), and the camera assembly. The slit assembly is mounted on the central flange, which acts as the only mechanical interface to the rocket skins. The telescope, spectrograph and camera are supported by thin-walled stainless tubes cantilevered from the central flange. The instrument tubes and optical mirrors are rotationally symmetric, which simplifies the alignment process.

The TMA and SOA (Figure 4) will be aligned and assembled at the Smithsonian Astrophysical Observatory. A Centroid Detector Assembly (CDA[7]) will be used to align each mirror relative to a reference mirror and to the mirrors bonded to the bonding pads in place. This procedure is especially critical for the relative alignment between the two spectrograph mirrors, whose alignment tolerance is 8 arcsec of tilt. The TMA and SOA also contain an alignment reticle for lateral alignment. The diffraction grating position and angle will be measured using a coordinate measuring machine and adjusted.

After the sub-assemblies are internally aligned to their reference mirror and reticle, the full instrument alignment will be performed by aligning these references to each other, so that the reticles lie on a line, and the reference mirrors perpendicular to that line. First, the TMA will be installed on the telescope tube, with a camera in place of the slit. The telescope focus is achieved through X-ray testing at the Stray Light Facility (SLF) at MSFC, a 100 m X-ray beamline. Correction will be made for the finite source distance.

Next, the slit and SOA will be installed at nominal separation, with their lateral position and tip/tilt angle aligned using conventional optical alignment techniques. Finally the camera will be installed, and the full system tested again at SLF to determine optimal camera position and to verify the end-to-end optical performance.

5. MIRROR DEVELOPMENT

The telescope and spectrograph mirrors are electroformed nickel replicated mirrors, currently being fabricated at MSFC. Sector mirrors made of polished glass were initially considered, but replicated mirrors were chosen because the axial symmetry of full cylindrical shells is a major advantage in aligning this complex instrument. Replicated mirrors are an established technology, successfully used on the Focusing Optics X-ray Solar Imager (FOXSI[8]) and other missions.

However, MaGIXS presents unique challenges not encountered on previous missions using replicated mirrors. The focal length is relatively short, and the shell length is long relative to the focal length: spectrograph mirrors have 562 mm focal length with a shell length of 80 mm, and the Wolter-I telescope mirror has a focal length of 1091 mm and a total (parabola + hyperbola) shell length of 250 mm. In other words, the sag (surface slope) is larger than a FOXSI-like replicated mirror, which makes metrology and figure tracking more challenging. In addition, achieving the end-to-end spectral resolution of 0.05 Å after 4 mirror reflections requires each mirror to have a 2.0 arcsecond spatial resolution, which is higher than previously achieved with this technique. Typically nickel replicated mirrors achieve 20 - 30 arcsecond resolution. This tight constraint is somewhat mitigated by the fact that the MaGIXS spectrograph only uses a small fraction (34 degrees of arc) of the mirror aperture.

Both mandrels were fabricated, polished and replicated, and their child mirror shells tested in X-ray before, and after Ir coating was depositited. For the single-paraboloid spectrometer mirrors, the resolution predicted

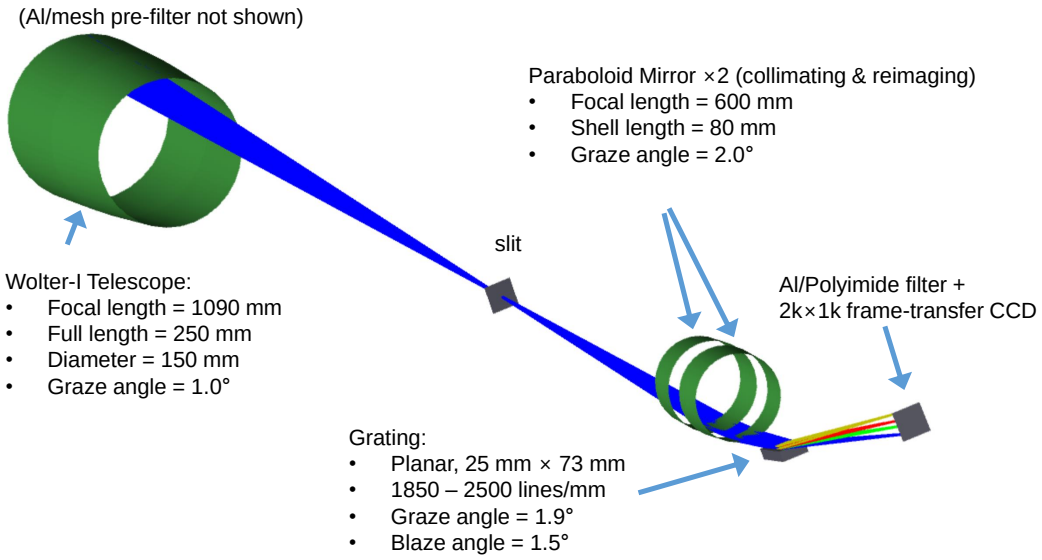

Figure 2. A slit spectrograph is necessary to obtain a dispersed spectrum of multiple points across a solar active region. MaGIXS is a fully grazing-incidence design, consists of a conventional Wolter-I telescope, a slit, and a spectrograph consisting of two parabolic mirrors and a flat varied line space grating. The two spectrograph mirrors are necessary to correct for coma and achieve the required spatial and spectral resolution throughout the length of the slit.

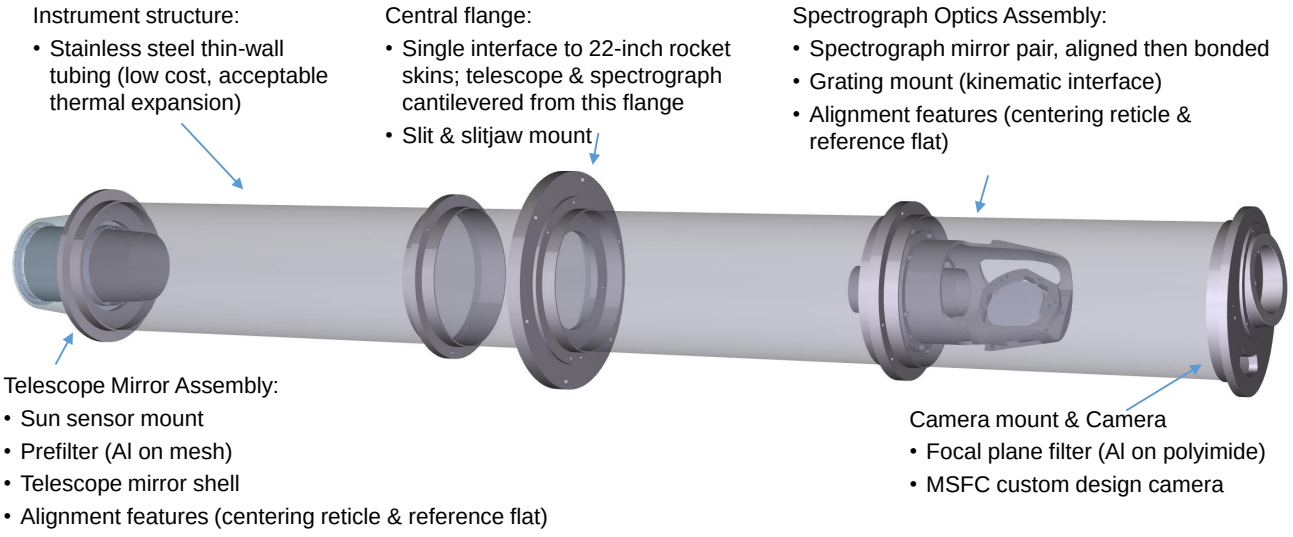

Figure 3. The MaGIXS instrument structure is cantilevered from a central flange, which is the only interface to the rocket skins. The structures are thin-wall stainless tubes.

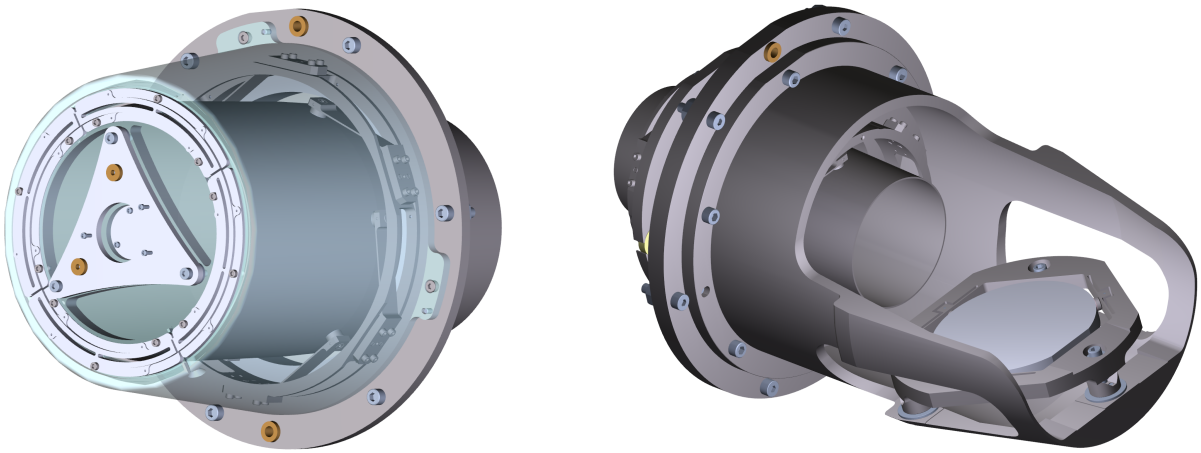

Figure 4. Mechanical designs for the Telescope Mirror Assembly (TMA, left) and Spectrograph Mirror Assembly (SOA, right). The TMA contains the Wolter-I telescope mirror shell, prefilters, mounting point for the sun sensor (not shown) and a light-tight shield. The SOA contains two paraboloid mirrors and the grating on a kinematic mount.

from metrology on the mandrel was about 17 arcseconds, half-power-diameter (HPD) (figure 5). A set of three spectrometer mirrors were tested in soft X-ray at MSFC's Stray Light Facility, using a Manson X-ray source with an aluminum target. At the characteristic Al K_α line (1.49 keV, 8.3 Å) the measured HPD was $\sim$ 23 arcseconds. Figure 5 shows the measured axial figure error of the spectrometer mandrel before and after lap polishing, and figure 6 is an X-ray image of the PSF produced by the spectrometer mirror (left) and a 3D rendering of the modeled PSF (right).

Since lap polishing methods alone have demonstrated to be insufficient for achieving precise, sub-arcsecond figure, the mandrels will be re polished using deterministic polishing techniques afforded by the *Zeeko Intelligent Robotic Polisher*. Recently, the *Zeeko* polishing process, developed at MSFC, has been tested and refined using a surrogate mandrel, which is identical to the flight telescope mandrel, but is not capable of being replicated. Initial results indicate that RMS slope error and corresponding resolution estimates can be achieved at the level required by MaGIXS. Figure 7 shows the axial figure error of the paraboloid segment of the surrogate mandrel before (black curve) and after deterministic polishing (gray curve). The predicted resolution dropped from $\sim$ 7.6 to $\sim$ 2.7 arcseconds, a 64% improvement in resolution. This method is yielding promising results, and soon we expect to achieve $\leq$ 0.7 arcsecond RMS slope error per segment ($\sim$ 1.9 arcsecond HPD), with the flight mandrel. Currently, the flight mandrels are being polished using the *Zeeko* and shells are scheduled to be replicated in July 2018 and tested in X-ray in August 2018.

6. OPTOMECHANICS DEVELOPMENT

The MaGIXS mirror mounts and grating mount have been designed by the Smithsonian Astrophysical Observatory, based on experience from Hinode/XRT, SDO/AIA, and other relevant missions.

The telescope mirror shell, a single shell containing both the hyperboloid and paraboloid sections of the Wolter Type-1 telescope, is supported by 6 flexures, bonded to the mirror shells at their centers of mass. While some amount of print-through is expected at the bond pads, analysis shows that these are localized around each bonding pad. The MaGIXS spectrograph only uses a small sector of the annular mirror aperture, and the bonding pads will be placed away from the spectrograph aperture.

The spectrograph mirror mounts are similar to the telescope mounts, with the added complexity of a strict tip/tilt relative angle requirement. The mirrors will be aligned optically prior to bonding. The grating will be bonded to a kinematic mount.

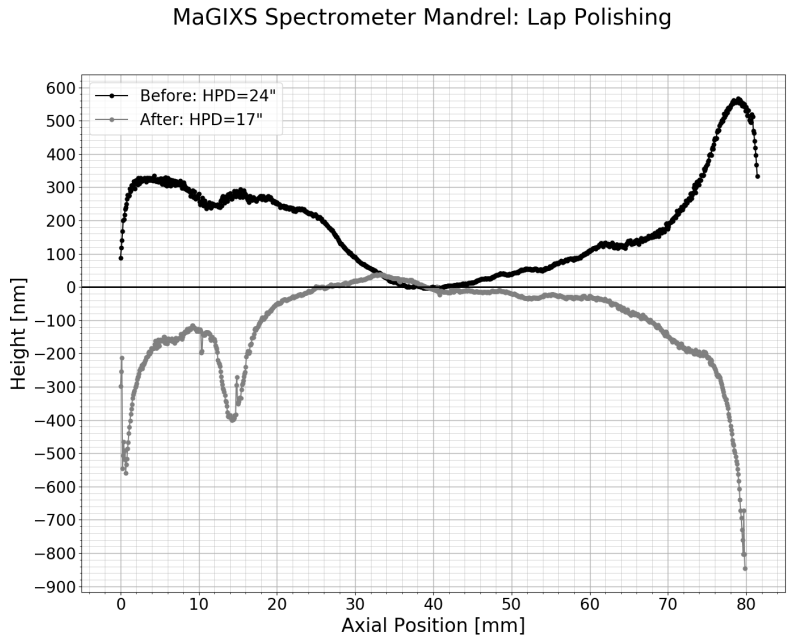

Figure 5. Axial figure error of the single-paraboloid spectrometer mandrel post-removal of diamond turning marks (black curve) and after completion of hand and lap polishing (gray curve). The predicted mandrel HPD after polishing is 17 arcseconds. Axial figure error is measured using a Zygo interferometer with a transmission flat. The result is a thin (0.5 mm) cross section of the mandrel in the axial direction.

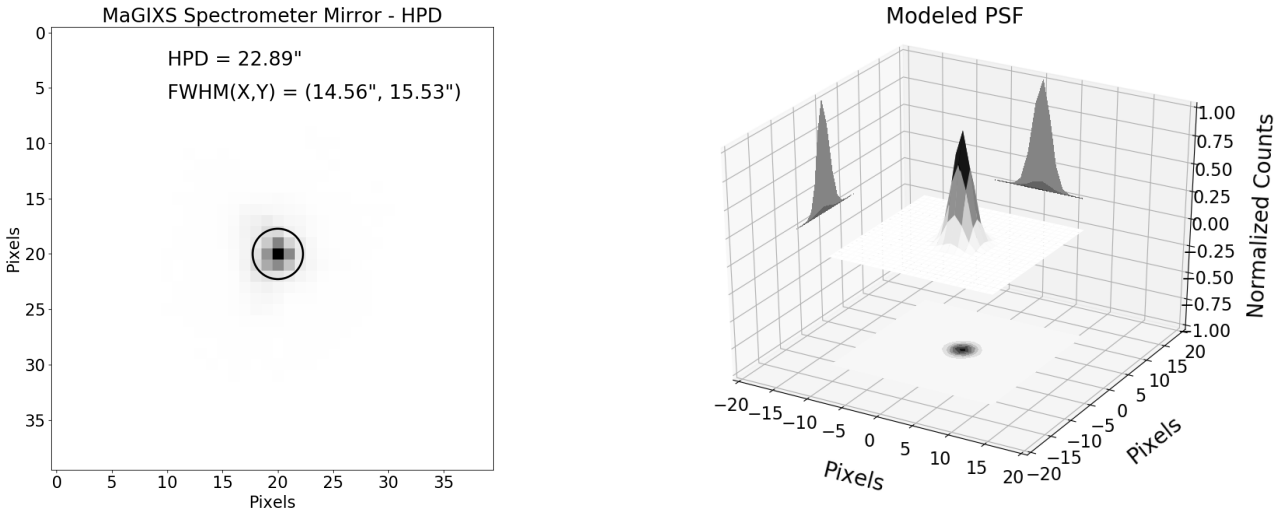

Figure 6. X-ray test of a replicated spectrometer mirror. *Left*: an X-ray image of the point source, with an over plotted circle representing the half-power-diameter. The FWHM in X, Y differ by about 1 arcsecond, suggesting that PSF is reasonably symmetric. *Right*: the 2D Gaussian model of the PSF, fitted using a least-squares fit.

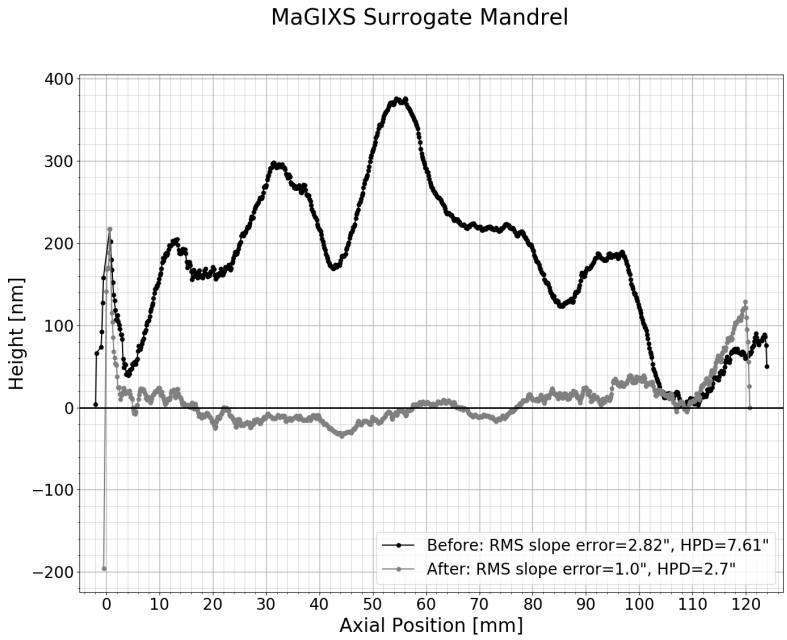

Figure 7. Axial figure error of the paraboloid segment of the surrogate mandrel post-removal of diamond turning marks (black curve) and after completion of *Zeeko* polishing (gray curve). The predicted mandrel HPD after polishing is 2.7 arcseconds. Note the gray curve does not represent our limit for figure correction - this effort was truncated here, to begin polishing the flight mandrel.

7. DIFFRACTION GRATING DEVELOPMENT

The MaGIXS reflection grating is being fabricated on a silicon substrate patterned via electron-beam lithography and etched by KOH (potassium hydroxide). The silicon substrate is 100 mm diameter, ultrapure float zone, {111} crystal orientation, custom offcut at 1.6 degrees toward the <211> flat. To achieve the desired flatness of 100 nm peak-to-valley, the samples are 10 mm-thick, and ground and polished. A 30 nm-thick layer of wet thermal SiO2 is grown on the substrate to mask the KOH. The period of the grating varies from 398 to 541 nm over a span of 73 mm. The grating is patterned via electron-beam lithography in positive-tone ZEP resist to achieve the desired variable line spacing. The pattern is transferred into the SiO2 layer via reactive-ion etching with CF4. The key step is to etch a 1.6 degree sawtooth profile into the grating via KOH, masked with SiO2. The {111} planes can be used as an etch stop in KOH since the etch rate of the non-{111} planes is ∼100x faster than the {111} planes. After the sawtooth is etched, the SiO2 mask is stripped in hydrofluoric acid and the grating can be coated in gold to maximize X-ray reflectivity.

8. CAMERA AND ELECTRONICS

The camera and avionics for MaGIXS are based on designs already flown on various MSFC sounding rocket experiments. The camera was originally developed for the reflight of the High Resolution Coronal Imager[9] sounding rocket experiment. The camera contains an e2v CCD230-42 2k×2k charge-coupled device (CCD); for MaGIXS, the CCD will be operated in 1k×2k frame-transfer mode. The camera has a 500 kpixel/s readout rate through each of the 4 readout taps, and has demonstrated ≈ 7 e- rms noise. The CCD is cooled to operating temperature using liquid nitrogen prior to launch.

The images are transferred to a flight computer via a SpaceWire connection. The flight computer is a military off-the-shelf single-board computer. All images are stored onboard as well as downlinked in near real-time.

9. SLITJAW IMAGER

A slitjaw imager is essential for determining the exact position of the slit on the Sun, so that the spectrum can be put in context and compared directly with concurrent observations. However, a reflective slit must be near-normal incidence, and thus cannot reflect the same soft X-ray energy range as the spectrograph. UV or EUV reflective coatings are a possibility, but necessitate UV/EUV re-imaging optics that are difficult to align and test.

Our solution is to directly apply a Lumogen phosphor coating onto the slit substrate to act as a broadband EUV/UV imaging screen. An off-the-shelf video camera with an optical macro lens is used to image the phosphor surface.

ACKNOWLEDGMENTS

This work is funded by the Low Cost Access to Space in NASAs Heliophysics Technology and Instrument Development for Science program.

REFERENCES

[1] Culhane, J. L., Bentley, R. D., Hiei, E., Watanabe, T., Doschek, G. A., Brown, C. M., Cruise, A. M., Lang, J., Ogawara, Y., and Uchida, Y., "The Bragg Crystal Spectrometer for Solar-A," Sol. Phys. **136**, 89–104 (Nov. 1991).

[2] Doschek, G. A. and Feldman, U., "TOPICAL REVIEW The solar UV-x-ray spectrum from 1.5 to 2000 Å," *Journal of Physics B Atomic Molecular Physics* **43**, 232001 (Dec. 2010).

[3] Golub, L., Deluca, E., Austin, G., Bookbinder, J., Caldwell, D., Cheimets, P., Cirtain, J., Cosmo, M., Reid, P., Sette, A., Weber, M., Sakao, T., Kano, R., Shibasaki, K., Hara, H., Tsuneta, S., Kumagai, K., Tamura, T., Shimojo, M., McCracken, J., Carpenter, J., Haight, H., Siler, R., Wright, E., Tucker, J., Rutledge, H., Barbera, M., Peres, G., and Varisco, S., "The X-Ray Telescope (XRT) for the Hinode Mission," Sol. Phys. **243**, 63–86 (June 2007).

[4] Culhane, J. L., Harra, L. K., James, A. M., Al-Janabi, K., Bradley, L. J., Chaudry, R. A., Rees, K., Tandy, J. A., Thomas, P., Whillock, M. C. R., Winter, B., Doschek, G. A., Korendyke, C. M., Brown, C. M., Myers, S., Mariska, J., Seely, J., Lang, J., Kent, B. J., Shaughnessy, B. M., Young, P. R., Simnett, G. M., Castelli, C. M., Mahmoud, S., Mapson-Menard, H., Probyn, B. J., Thomas, R. J., Davila, J., Dere, K., Windt, D., Shea, J., Hagood, R., Moye, R., Hara, H., Watanabe, T., Matsuzaki, K., Kosugi, T., Hansteen, V., and Wikstol, Ø., "The EUV Imaging Spectrometer for Hinode," Sol. Phys. **243**, 19–61 (June 2007).

[5] Winebarger, A. R., Warren, H. P., Schmelz, J. T., Cirtain, J., Mulu-Moore, F., Golub, L., and Kobayashi, K., "Defining the "Blind Spot" of Hinode EIS and XRT Temperature Measurements," ApJ **746**, L17 (Feb. 2012).

[6] Kobayashi, K., Cirtain, J., Golub, L., Korreck, K., Cheimets, P., Hertz, E., and Caldwell, D., "Stigmatic grazing-incidence x-ray spectrograph for solar coronal observations," *Proc. SPIE* **7732**, 33 (July 2010).

[7] Glenn, P. E., "Centroid detector assembly for the AXAF-I alignment test system," Proc. SPIE **2515**, 352–360 (June 1995).

[8] Krucker, S., Christe, S., Glesener, L., Ishikawa, S.-n., Ramsey, B., Takahashi, T., Watanabe, S., Saito, S., Gubarev, M., Kilaru, K., Tajima, H., Tanaka, T., Turin, P., McBride, S., Glaser, D., Fermin, J., White, S., and Lin, R., "First Images from the Focusing Optics X-Ray Solar Imager," ApJ **793**, L32 (Oct. 2014).

[9] Kobayashi, K., Cirtain, J., Winebarger, A. R., Korreck, K., Golub, L., Walsh, R. W., De Pontieu, B., DeForest, C., Title, A., Kuzin, S., Savage, S., Beabout, D., Beabout, B., Podgorski, W., Caldwell, D., McCracken, K., Ordway, M., Bergner, H., Gates, R., McKillop, S., Cheimets, P., Platt, S., Mitchell, N., and Windt, D., "The High-Resolution Coronal Imager (Hi-C)," Sol. Phys. **289**, 4393–4412 (Nov. 2014).